Published in final edited form as:
J Neurochem. 2009 August ; 110(3): 857–869. doi:10.1111/j.1471-4159.2009.06173.x.

Selective astrocytic gap junctional trafficking of molecules involved in the glycolytic pathway: Impact on cellular brain imaging

Gautam K. Gandhi[a], **Nancy F. Cruz**[b], **Kelly K. Ball**[b], **Sue A. Theus**[c], and **Gerald A. Dienel**[a,b]

[a]Department of Physiology and Biophysics, UAMS, Little Rock, Arkansas, 72205, USA

[b]Department of Neurology, University of Arkansas for Medical Sciences, Little Rock, Arkansas, 72205, USA

[c]Central Arkansas Veterans Health Systems and Department of Pathology, UAMS, Little Rock, Arkansas, 72205, USA

Abstract

To assess the specificity of metabolite trafficking among gap junction-coupled astrocytes, we developed novel, real-time, single-cell enzymatic fluorescence assays to assay cell-to-cell transfer of unlabeled glycolytic intermediates and report (i) highly restricted transfer of glucose-6-phosphate (P) and two analogs, deoxyglucose-6-P (DG-6-P), and 2-NBDG-6-P, compared to DG and 2- and 6-NBDG, (ii) extensive junctional diffusion of glyceraldehyde-3-P, NADH, and NADPH plus three anionic fluorescent dyes used as internal standards for transfer assays, and (iii) stimulation of gap junctional communication by increased intracellular Na^+ that also evokes metabolic responses in nearby coupled astrocytes. Thus, dye transfer does not predict gap junctional permeability of endogenous metabolites. Intracellular retention of flux-regulating compounds (e.g., glucose-6-P) may be necessary for local metabolic control, whereas 'syncytial sharing' may dissipate the work load on peri-synaptic astrocytes. Imaging of brain functional activity depends on local accumulation of exogenous or endogenous signals, and DG-6-P is trapped in the cell where it is phosphorylated, whereas rapid dispersal of cytoplasmic NAD(P)H and labeled glucose metabolites throughout the astrocytic syncytium can interfere with cellular assessment of neuron-astrocyte relationships in autoradiographic, fluorescence microscopic, and magnetic resonance spectroscopic studies.

Keywords

astrocyte; connexin; gap junction; hexose-6-phosphate; NAD(P)H fluorescence; brain imaging

The 'tripartite synapse' is comprised of pre- and post-synaptic neuronal and peri-synaptic astrocytic structures (Araque *et al*. 1999) with heterogeneous coupling of astrocytes via gap junctions to form syncytia comprised of as many as ten thousand cells in the rat inferior colliculus (Ball *et al*. 2007 and cited references). Functions and regulation of astrocytic syncytia are poorly understood (Tabernaro *et al*. 2006), but small molecule diffusion may help coordinate long-range astrocyte-neuron signaling via second messengers, nutrient delivery,

Corresponding Author: Gerald A. Dienel, Ph.D., University of Arkansas for Medical Sciences, Department of Neurology, Slot 830, Shorey Building, Room 715, 4301 West Markham Street, Little Rock, AR 72205, Phone (501) 603-1167, Fax (501) 296-1495, gadienel@uams.edu.

COMPETING FINANCIAL INTERESTS
The authors declare that they have no competing financial interests.

enhanced energy production, and dispersal of ions and lactate. Astrocytes have key roles in brain function including extracellular ion buffering, de novo synthesis of neurotransmitters, transmitter uptake from the synaptic cleft, communication between vasculature and neurons, and responses to injury (Voltera *et al*. 2005; Hertz *et al*. 2007). Astrocytes form syncytial networks via intercellular channels comprised of connexin (Cx) proteins, Cx43, Cx30, and Cx 26 (Nagy *et al*. 2004). These channels are widely believed to mediate relatively unrestricted intercellular exchange of cytoplasmic molecules smaller than ~1 kDa, yet exhibit preferential transfer that is governed by size, charge, and connexin composition (Harris 2007). Impairment of gap junctional communication causes deafness (Beltramello *et al.* 2005) and increases neuronal vulnerability to excitatory damage (Zündorf *et al*. 2007), underscoring its importance in brain function.

Astrocytes are widely believed, but not proven, to consume most of the glucose during brain activation, and determination of cellular contributions to metabolic brain images obtained during activation with glucose utilization tracers is an important, unresolved research area (Dienel and Cruz 2008). Monotonic acoustic stimulation elicits tonotopic bands of metabolic activation in the inferior colliculus (Cruz *et al*. 2007), an auditory structure that has the highest blood flow and glucose utilization rates in brain (Gross *et al*. 1987) and extensively-coupled astrocytes (Ball *et al*. 2007). Because hexose-6-phosphates(P) are reported to be transferred through gap junction channels (Finbow and Pitts 1981; Tabernaro *et al*. 1996) zones of focal activation should quickly dissipate when imaged with [^{14}C]deoxyglucose (DG) due to rapid spreading of its primary metabolite, [^{14}C]DG-6-P, throughout the extensive astrocytic syncytium. Unexpectedly, we found that focal activation is readily visualized with [^{14}C]DG but not with [1- or 6-^{14}C]glucose, due, in part, to gap junction-mediated dispersal and release of labeled glucose metabolites (Ball *et al*. 2007; Cruz *et al*. 2007; Dienel and Cruz 2008). These results suggest that neurons may consume most of the glucose (and DG) or that DG-6-P does not readily pass through gap junctional channels. To address this issue, gap junctional transfer of glycolytic intermediates (Fig. 1a) was assayed in cultured astrocytes and adult brain slices using three analytical approaches, (i) real-time imaging of cellular labeling by fluorescent glucose analogs, (ii) autoradiographic imaging of deoxyglucose label spread, and (iii) novel, fluorescent single-cell enzymatic assays with high specificity and sensitivity for unlabeled biological molecules.

MATERIALS AND METHODS

Reagents

Dulbecco's modified Eagle's medium (DMEM, Catalog # 12320-032), penicillin, streptomycin, Amphotericin B, and trypsin were obtained from Invitrogen (Carlsbad, CA). Fetal bovine serum (FBS) was purchased from Hyclone (Logan, UT). Dibutyryl cyclic-adenosine monophosphate (dBcAMP), L-leucine methyl ester hydrochloride (L-LME), octanol, cytochalasin B, Evan's Blue, bovine serum albumin, Lucifer yellow VS (dilithium salt), microtubule associated protein 2 (MAP2) antibody, NAD^+, $NADP^+$, NADH (sodium or potassium salt), NADPH (sodium salt), glucose-6-phosphate, glyceraldehyde-3-phosphate, glucose-6-phosphate dehydrogenase from Torula yeast, glyceraldehyde-3-phosphate dehydrogenase from rabbit muscle, phosphoglycerate kinase from baker's yeast, ADP, and ATP were from Sigma-Aldrich (St. Louis, MO). Antibody against S100β was from DakoCytomation (Carpinteria, CA), D-hexose-6-phosphotransferase from yeast (hexokinase) from Roche (Indianapolis, IN), and 2-deoxy-D-[1,2-^{3}H]glucose ([^{3}H]DG, 27.4 Ci/mmol) from PerkinElmer Life Sciences (Boston, MA). FITC-conjugated dextran, 2-(*N*-(7-nitrobenz-2-oxa-1,3-diazol-4-yl)amino)-2-deoxyglucose (2-NBDG), 6-(N-(7-nitrobenz-2-oxa-1,3-diazol-4-yl)amino)-6-deoxyglucose (6-NBDG), Alexa Fluor 350 carboxylic acid,

succinimidyl ester (A350), Alexa Fluor 568 (A568), sulforhodamine 101 (SR101), and Texas red hydrazide (TxRed hyd) were from Invitrogen (Molecular Probes, Eugene, OR).

Synthesis of 2-NBDG-6-phosphate(P) and [^{3}H]DG-6-P

2-NBDG (20 mmol/L) was incubated in reaction mixtures containing 22 mmol/L ATP, 22 mmol/L $MgCl_2$, and 10 mmol/L HEPES, pH 7.3 in the presence or absence of hexokinase (22.5 U/ml) at 37°C for 1 hour. The time for complete conversion of 2-NBDG to 2-NBDG-6-P was established by thin-layer chromatographic separation of precursor and product; after completion of derivatization, the hexokinase-containing mixture contains 20 mmol/L 2-NBDG-6-P, 20 mmol/L ADP, and 2 mmol/L ATP plus the other components; that without enzyme contains the starting materials.

[^{3}H]DG (5 mCi/ml or 0.18 mmol/L, based on its specific activity) was incubated in the presence or absence of hexokinase using the same mixture described above, except that the ATP and $MgCl_2$ concentrations were reduced to 0.5 mmol/L. The time required for complete phosphorylation of [^{3}H]DG was determined in a parallel assay by measuring the fall in the concentration of unlabeled glucose (Biochemistry Analyzer, Yellow Springs Instruments, Yellow Springs, OH); because glucose is a better substrate for hexokinase, the reaction time for [^{3}H]DG was doubled. After the hexokinase reaction was complete, 0.18 mmol/L of [^{3}H]DG-6-P and ADP are formed and 0.32 mmol/L ATP remains; a portion of the reaction mixture was assayed by anion exchange column chromatography to verify phosphorylation of virtually all of the [^{3}H]DG. Unlabeled glucose was then added to all mixtures at a final concentration of 3 mmol/L as a carrier to compete for any non-specific binding of ^{3}H-labeled compounds (carrier glucose was not added to the NBDG assays due to its 100-fold higher concentration). This addition results in consumption of all of the remaining ATP in the hexokinase-containing reaction mixtures to form final concentrations of 0.5 mmol/L ADP, 0.32 mmol/L glucose-6-P (Glc6P), and 2.68 mmol/L glucose. [^{3}H]DG mixtures that did not contain hexokinase contain the starting concentrations of DG and ATP plus carrier glucose.

To simplify the assays, phosphorylated hexoses were not purified from reaction mixture components; test reaction mixtures were diffused directly into single astrocytes. The difference between the test solutions containing precursor and phosphorylated product was the presence or absence of hexokinase and the amounts of ATP, ADP, glucose, and Glc-6-P. Because the pipette solution (see below) contained 2 mmol/L ATP, the 2-NBDG solution had 24 mmol/L ATP and no ADP, whereas all other solutions contained different amounts of ADP; the ATP/ADP ratios (a measure of cellular energy status) for the 2-NBDG-6-P, [^{3}H]DG, and [^{3}H]DG-6-P injection solutions are calculated to be 0.2, 4, and 6.25, respectively.

Cell culture

Cultured astrocytes were prepared by small modifications of established procedures (Hertz *et al*. 1998). Briefly, astrocytes were harvested from cerebral cortex of 1-day-old albino Wistar-Hanover rats (Taconic Farms, Germantown, NY) and grown in T-75 culture flasks with DMEM containing 5.5 mmol/L glucose, 10% FBS, 50 IU of penicillin, and 50 μg/ml of streptomycin at 37°C in humidified air containing 5% CO_2. L-LME (0.1 mmol/L), a lysosomotrophic agent that selectively destroys mononuclear cells including microglia, was also included in the culture medium, and the cultures were shaken by hand weekly to remove microglia. When confluent, the cells were trypsinized, seeded onto polylysine-coated glass coverslips, and grown to confluence in medium containing Amphotericin B (2.5 μg/mL); then differentiation was induced by supplementing the culture medium with 0.25 mmol/L dBcAMP and cells maintained for at least 2 weeks. Purity of cultures was based on expression of the astrocyte marker, glial fibrillary acidic protein, which was expressed in >90% of the cells.

Brain slice preparation

Adult male Wistar-Hanover rats (300-350g) were anesthetized with halothane and their brains were quickly removed and chilled by immersion in oxygenated, ice-cold artificial cerebral spinal fluid (aCSF) solution containing 26 mmol/L $NaHCO_3$ (pH 7.3) and 248 mmol/L sucrose, and 250 μm-thick slices were prepared as described (Moyer and Brown 1998). Coronal sections of midbrain (including inferior colliculus) were cut using a Leica (Heidelberg, Germany) VT 1000S tissue slicer, inferior colliculus slices were incubated in oxygenated aCSF containing sucrose for 30 minutes at 35°C, then for 1 h at 22°C, and transferred to an open bath perfusion chamber (Warner Instruments, Hamden, CT) for intracellular injection studies (Moyer and Brown 1998).

Identification of sulforhodamine 101 (SR101)-positive cells as astrocytes in slices of adult rat inferior colliculus

SR101 is a specific marker for astrocytes in the cerebral cortex but not in the cerebellum (Nimmerjahn *et al*. 2004). To establish that $SR101^+$ cells in slices of inferior colliculus are highly coupled by gap junctions, slices were incubated in SR101 (250 nmol/L), single SR101-labeled cells impaled with a micropipette containing Lucifer yellow, and co-registration of the two dye markers was assessed. To compare cellular localization of SR101 and cell type markers, separate groups of slices were incubated in 500 nmol/L Texas Red hydrazide (a fixable derivative of SR101) for 5 minutes, slices were washed with oxygenated perfusion solution (see below), then immediately immersed in and quickly mixed with 10 mL of freshly-prepared 4% paraformaldehyde in 0.1 mol/L phosphate-buffered saline, pH 7.2-7.3 at room temperature, followed by gentle mixing on a platform shaker for 24 h. Then 7 μm-thick serial sections of the slices were cut and immunostained for the calcium binding protein S100β (1:1000 dilution), an astrocyte marker, or MAP2 (1:1000 dilution), a neuronal marker, as previously described (Ball *et al*. 2007). Images for analysis of co-localization were taken with a Nikon E600 microscope and analyzed with MetaVue software.

Gap junction dye transfer assays

Micropipettes with 12-14 MΩ resistance (tip inner diameter: 1.00 ± 0.13 μm, outer diameter: 1.82 ± 0.14 μm; means ± SD, n=5) were constructed from borosilicate glass (1 mm OD, 0.5 mm ID) using a P97 pipette puller (Sutter Instruments, Novato, CA) and filled with a test solutions containing fluorescent or radioactive probes, alone or in various combinations. Except where noted, micropipette solutions contained (composition in mmol/L) 21.4 KCl, 0.5 $CaCl_2$, 2 $MgCl_2$, 5 EGTA, 2 ATP, 0.5 GTP, 2 ascorbate, 10 HEPES, pH 7.2, fluorescent (6-NBDG, 2-NBDG, 2-NBDG-6-P, NADH or NADPH) or radiolabeled ([^{3}H]DG or [^{3}H]DG-6-P) tracers, and internal standards to label the injected cell and gap junction-coupled cells. Fluorescence was determined before (background) and 10 min after diffusion of the test compound into a single astrocyte. Non-permeant macromolecules to identify the impaled cell were FITC-conjugated dextran (molecular weight, 40,000 Da) or Evan's Blue Albumin (>66,000 Da), a dye that is protein bound at a ratio of 1% weight/volume Evan's Blue plus 5% bovine serum albumin. Lucifer yellow VS (4%; 536 Da when ionized excitation/emission maxima: 430/530 nm) was the internal standard for assays with [^{3}H]DG (166 Da) and [^{3}H] DG-6-P (196 Da). Due to spectral overlap of Lucifer yellow VS and NBDG (475/550 nm), Alexa Fluor 350 (5 mmol/L; 346/442 nm; 311 Da when ionized after the succinimidyl ester is hydrolyzed by water to form the carboxylic acid) was the internal standard for the assays with 6- and 2-NBDG (20 mmol/L; 342 Da) and 2-NBDG-6-P (20 mmol/L; 372 Da). Alexa Fluor 568 (5 mmol/L; 578/603 nm; 730 Da) was the internal standard for NADH and NADPH (25 mmol/L; 340/460 nm; 663 and 723 Da, respectively) transfer assays. The osmolarity of each solution was measured (Osmette II, Precision Systems, Natick MA) and adjusted to 305-320 mOsm/L with sucrose. Preliminary studies showed that the areas labeled by Lucifer yellow

VS dissolved in 300 or 400 mOsm/L solutions were similar in 10 min diffusion assays (not shown), indicating that small differences (<10%) in osmolarity of pipette solutions that can cause astrocyte swelling are unlikely to alter area labeled by gap junctional diffusion.

Cultured astrocytes and inferior colliculus slices from adult rat brain were transferred to the microscope stage and perfused (1 ml/min) with aCSF containing 26 mmol/L $NaHCO_3$ (pH 7.3), 10 μmol/L cytochalasin B, 10 mmol/L glucose, and 10 mmol/L pyruvate. All assays of hexose gap junctional transfer employed cytochalasin B, a glucose transport inhibitor (Speizer et al. 1985), to minimize hexose efflux from cells via glucose transporters after microinjection (see Results, Table 1). The perfusion medium was supplemented with 10 mmol/L glucose to compete for re-uptake of any tracer that may leak out of cells; pyruvate (10 mmol/L) was added as an oxidative fuel to compensate for glucose transport blockade. Perfusion solutions were freshly prepared, kept at room temperature, and continuously bubbled with O_2/CO_2 (95/5%).

Cultured astrocytes were visualized under differential interference contrast (DIC) with a Nikon Eclipse E600 microscope (Melville, NY) using a Photometrics CoolSNAP ES camera (Roper Scientific, Atlanta, GA) and MetaVue software (Molecular Devices, Sunnyvale, CA); those in inferior colliculus slices were identified by specific labeling by SR101. Astrocytes were impaled with micropipettes using a MP-225 manipulator (Sutter Instruments, San Francisco, CA), and tracers diffused into cells for 10 min before the micropipette was removed. Gap junctional transfer was inhibited by pretreatment with 0.6 mmol/L octanol. Fluorescence intensity and area labeled by fluorescent probes were with MetaVue software.

The area labeled by [^{3}H]tracers was determined by autoradiography and computer-assisted densitometry (MCID™) (InterFocus Imaging Ltd., Linton, Cambridge, England). Immediately after the 10 min diffusion interval, the coverslips containing the cultured astrocytes were quickly washed twice by sequential dipping into two fresh perfusion solutions containing 10 μmol/L cytochalasin B, followed by blotting one edge of the coverslip against absorbent filter paper to drain the adhering liquid and dried on a slide warmer at 55°C. The brain slices were removed from the perfusion chamber, rinsed twice as above, placed flat on tin foil, frozen in isopentane at ~ -40°C and stored at -80°C until cut into 7 μm-thick sections; the serial tissue sections were collected on cover slips and dried as above. All cell and tissue samples were exposed to Kodak BioMax MR-1 or Hyperfilm tritium (GE Healthcare Bio-sciences Corp. Piscataway, NJ) X-ray film for 4-6 months, and ^{3}H labeled areas determined in each section and summed. Because the film had a protective coating, registration of ^{3}H is reduced, and measured areas may be underestimated because the outermost syncytial boundaries would have the lowest tracer levels.

"Hemichannel"/pannexin pore assays

Cultured astrocytes were incubated with 2-NBDG (0.4 mmol/L in culture medium in the CO_2 incubator at 37°C) to accumulate NBDG-6-P inside the cells. Cells were removed from the incubator, transferred to the microscope stage, perfused with aCSF for 5 min, and zero time NBDG-6-P fluorescence was assayed. Perfusion was continued with aCSF containing or omitting divalent cations; extracellular medium nominally lacking Ca^{2+} and Mg^{2+}divalent cations opens "hemichannels" (Ye *et al*. 2003) and $P2X_7$ receptor-linked pannexin pores (Suadicani *et al*. 2006; Iglesias *et al*. 2008). After 25 min perfusion, NBDG-6-P fluorescence was measured and percent change was calculated (100*ΔF/F). Then the same cells were exposed to 1 mmol/L Lucifer yellow in the respective aCSF (± divalent cations) followed by 20 min perfusion wash with Ca^{2+}-Mg^{2+} aCSF, and the net change in Lucifer yellow fluorescence was determined.

Single-cell, fluorescence-linked enzyme assays for gap junctional transfer of endogenous metabolites

In brief, the principle of these assays is to insert an NAD(P)-linked dehydrogenase assay mixture plus a permeant fluorescent dye into one astrocyte to identify a second dye-coupled astrocyte into which a test compound is inserted. If the compound diffuses through gap junctions into the reporter astrocyte, its oxidation generates a fluorescent product, NAD(P)H. Gap junctional transfer of glucose-6-phosphate (Glc-6-P) was assayed using Glc-6-P dehydrogenase (DH) to convert $NADP^+$ and Glc-6-P to NADPH plus 6-phosphoglucono-δ-lactone; spontaneous hydrolysis of the lactone to 6-phosphogluconate makes the reaction irreversible. The enzyme assay system diffused into the reporter astrocyte consists of 62.5 units/ml Glc-6-P DH, 25 mmol/L $NADP^+$, 10 HEPES (pH 7.5), and 5 mmol/L A568; 5 mmol/L Glc-6-P was diffused into the donor astrocyte. Glyceraldehyde-3-phosphate (GAP) transfer was assayed using GAP DH to convert NAD^+ and GAP to NADH plus 1,3-bisphosphoglycerate. To compensate for an unfavorable equilibrium for this reaction, phosphoglycerate kinase (PGK) and ADP were included in the reaction mixture to pull the reaction in the direction of NADH formation by converting 1,3-bisphosphoglycerate to 3-phosphoglycerate plus ATP. The reporter system consisted of 120 units/ml of GAP dehydrogenase and 274 units/ml PGK in the reaction mixture containing (in mmol/L), 19.1 NAD^+, 19.1 Na-ADP, 19.1 KPO_4, 10 HEPES (pH 7.5), and 5 A568; the donor astrocyte received 5 mmol/L glyceraldehyde-3-phosphate.

Statistics

All statistical analyses were performed with SAS software, version 6.12 (SAS Institute Inc., Cary, NC). Comparisons between two groups of independent samples were made with two-tailed, unpaired t tests. Comparisons among 3 or more groups of independent samples were made with one-way ANOVA and Tukey's test. In some experiments, the variability of gap junctional communication was taken into account by comparisons of normalized areas, i.e., the area labeled by a test compound in each impaled cell was divided by that labeled by the permeant internal standard fluorescent dye obtained in that cell; these ratio data were transformed, i.e., ln((test area/dye area) +1) prior to statistical analyses. Reported values are means; vertical error bars in figures represent 1 SD.

RESULTS

Fluorescent glucose analogs

First, trafficking of two commercially-available fluorescent glucose analogs, 6-NBDG and 2-NBDG, was compared; 6-NBDG is not metabolizable, whereas 2-NBDG can be phosphorylated by endogenous hexokinase to form 2-NBDG-6-P (Aller *et al.* 1997; Speizer *et al.*1985). If hexose-6-P permeability through gap junctional channels were restricted, the area labeled by 2-NBDG would be smaller than that by 6-NBDG, and this prediction was confirmed in cultured astrocytes (Fig. 1b). For direct evaluation of the phosphorylated derivative, we enzymatically synthesized 2-NBDG-6-P and verified complete removal of the precursor, which is gap junction permeable and would interfere with the assay. Because transfer assays were carried out without removal of reaction mixture components, diffusion of the reaction mixture into an astrocyte would increase the level of ADP in impaled cells (see Methods) and reduce the intracellular ATP/ADP ratio, perhaps influencing AMP-mediated metabolic signaling and gating of gap junctional channels. Dye labeling was, however, similar when assayed in the presence of high ATP and ADP levels (Table 1). Note that inclusion of the glucose transporter inhibitor, cytochalasin B, in the perfusion solution was required to block transporter-mediated efflux of 2-NBDG from the coupled cells to the perfusion medium; in the absence of cytochalasin B, the area labeled by 2-NBDG fell by 55%, whereas labeling by Lucifer yellow and 2-NBDG-6-P was unaffected; Lucifer yellow labeling was 30% lower when

assayed in the presence of high ADP plus cytochalasin compared to low ATP + GTP in the absence of cytochalasin (Table 1).

When 2-NBDG and 2-NBDG-6-P were diffused into single astrocytes (Figs. 1c, d) 2-NBDG labeled an area 14.6-fold greater that of 2-NBDG-6-P (Fig. 1g, h, k) even though both groups of cells were well-coupled, based on labeling by the internal standard, Alexa Fluor 350 (Figs. 1e, f, k). Phosphorylation reduced 2-NBDG diffusion to that of Evan's blue-albumin, a non-permeant internal standard (Fig. 1h-k). Transfer of all permeant tracers was markedly reduced by octanol, a gap junction blocker (Fig. 1k).

Unapposed hemichannels and pannexin pores are normally tightly closed but can be opened by exposure of astrocytes to a medium nominally lacking divalent cations (Ye *et al*. 2003; Suadicani *et al*. 2006; Iglesias *et al*. 2008). To assess release via open hemichannels, astrocytes were incubated with 2-NBDG to generate intracellular 2-NBDG-6-P, subjected to a washout period to remove all unmetabolized NBDG, then perfused with normal or Ca^{2+}-Mg^{2+}-free artificial cerebrospinal fluid. Lack of divalent cations did not facilitate release of NBDG-6-P (Fig. 1l, left panels), but enabled uptake of bath-applied Lucifer yellow (Fig. 1l, right panels). Thus, restricted passage of NBDG-6-P is independent of pore formation between astrocytes.

Astrocytic gap junction connexin composition and properties may differ in mature brain compared to cultured cells, and 2-NBDG-6-P channel permeation was, therefore, tested in slices of adult inferior colliculus. Astrocytes were identified with Sulforhodamine 101 (SR101), a specific marker for cortical but not cerebellar astrocytes (Nimmerjahn *et al*. 2004). Use of SR101 as an astrocyte marker in the inferior colliculus was first established by demonstrating that SR101-positive cells are highly coupled when Lucifer yellow is diffused into a single cell (Fig. 2a-d) and that SR101 co-registers with an astrocyte marker, S100β, but not with a neuronal marker, MAP-2 (Fig. 2e-h). Diffusion of 2-NBDG into SR101-positive astrocytes revealed high dye coupling, labeling an area 13 times greater than that of 2-NBDG-6-P (Figs. 2i-k). Thus, 2-NBDG-6-P is a very poor substrate for gap junctional transfer in cultured cerebral cortical astrocytes and in adult rat inferior colliculus. Because the hydrophobic fluorescent moiety of NBDG and its larger size compared to glucose may influence binding to cellular components and passage through gap junctional channels transfer of smaller hexose-6-phosphates was tested next.

Radiolabeled glucose analogs

Radiolabeled DG is the 'gold standard' tracer to measure local rates of glucose utilization in brain due to trapping of DG-6-P (Sokoloff 1986), but the magnitude of focal activation would be underestimated if there were significant syncytial diffusion of DG-6-P (Finbow and Pitts 1981). To test this possibility, [^{3}H]DG-6-P was synthesized from [^{3}H]DG, and each tracer was inserted into single astrocytes along with Lucifer yellow. Dye-coupling was identical in the paired groups (Figs. 3d, f), but [^{3}H]DG diffusion was 4.1- and 16.7-fold greater than [^{3}H]DG-6-P in cultured astrocytes (Fig. 3a-c) and inferior colliculus slices (Fig. 3e), respectively; note that these values may be underestimated due to some [^{3}H]DG phosphorylation by endogenous hexokinase (Fig. 1b). Octanol markedly reduced the area labeled by [^{3}H]DG and Lucifer yellow (Fig. 3c-f).

Single cell enzymatic assays of gap junctional trafficking of unlabeled phosphorylated glycolytic intermediates

[^{14}C]Glucose-6-P was reported to be gap junction-permeable based on ^{14}C transfer assays (Tabernaro *et al*. 1996), contrasting our results above. However, rapid metabolism of [^{14}C] glucose-6-P by enzymes released during the scrape-loading procedure is likely, and the permeant [^{14}C]compounds were not identified (Tabernaro *et al*. 1996). To address this

discrepancy and to assay directly channel transfer of glucose-6-P, we developed novel, sensitive, specific single-cell $NAD(P)^+$-linked dehydrogenase enzyme assays to detect diffusion of unlabeled metabolites from donor to coupled recipient astrocytes (Fig. 4a). First, an astrocyte is visualized and impaled with a micropipette containing the glucose-6-P dehydrogenase reaction mixture plus Alexa Fluor 568 (Fig. 4c, pipette 1); the enzyme is retained in the reporter cell due to size, and dye transfer identifies coupled cells (Fig. 4b). Then, a second micropipette containing glucose-6-P is inserted into a coupled astrocyte located ~50 μm from the reporter (Fig 4c, pipette 2); if transferred, its enzymatic oxidation in the reporter cell produces fluorescent NADPH (Fig. 4a). When glucose-6-P was diffused into a coupled donor cell the net rise in fluorescence generated in the reporter cell was very small, similar to that of buffer (Fig. 4k), which is a control for metabolic responses to signals evoked by mechanical perturbation (e.g., Ca^{2+} waves or ATP release). Note that the reporter cell in Fig. 4f had higher fluorescence than neighboring and background cells (Fig. 4e), probably due to endogenous glucose-6-P derived from glucose and glycogen. To verify responsiveness of the enzymatic assay, the glucose-6-P containing pipette was then withdrawn from the initially-impaled cell and inserted into the reporter (denoted as ‘same’ cell, Figs. 4d, k). Then, the reporter cell fluorescence rose 12.7-fold above that obtained with a buffer-containing pipette (Figs. 4g, k). NADPH fluorescence also increased markedly in the reporter pipette (Fig. 4g) when both pipettes were in the same cell, but not when placed in separate coupled cells (Fig. 4f). Thus, glucose-6-P diffusion through gap junction channels is very low (Fig. 4f, g, k), and three independent approaches demonstrate that transfer of hexose-6-phosphates is highly restricted in both cultured and adult brain astrocytes.

All phosphorylated glycolytic intermediates are present in low concentrations in brain, raising the possibility that their diffusion through gap junctions may also be regulated to maintain optimal glycolytic flux within each astrocyte. To assay transfer of a representative triose-phosphate, glyceraldehyde-3-P (GAP), we devised a second micro-analytical assay system using a GAP dehydrogenase-phosphoglycerate kinase-coupled reaction. Glyceraldehyde-3-P readily diffused between coupled cells and stimulated a 28-fold higher increase in NADH fluorescence in the reporter cell (Fig. 4i) compared to the buffer control (Fig. 4l). Thus, selective gating of glycolytic intermediates is not simply due to the phosphate moiety or its net charge. When both donor and reporter pipettes were placed in the same cell, the response in the reporter cell tended to increase (Fig. 4j, l), and the fluorescence in the reporter pipette was greater during delivery of substrate to the same cell (Fig. 4j) compared to a coupled cell (Fig. 4i). Extracellular signaling did not contribute to NADH fluorescence because insertion of the substrate-containing pipette into a nearby non-coupled (i.e., not dye-labeled) astrocyte elicited a very small reporter response compared to that produced after removal of the pipette and insertion into the reporter cell (Fig. 4m, left panels) or into a coupled astrocyte (Fig. 4l, left panels). Octanol markedly reduced the substrate-dependent rise in NADH fluorescence without inhibiting the enzymatic reaction (Fig. 4m). NADH fluorescence was higher in coupled (Figs. 4i, j) compared to background cells (Fig. 4h), suggesting gap junctional transfer of metabolic signals or of NADH.

Redox trafficking

NADH and NADPH have essential roles in glycolytic flux and oxidative stress, and these redox molecules are used as endogenous ‘reporter molecules’ in fluorescence microscopic assays of cellular activity (Shuttleworth *et al.* 2003; Kasischke *et al.* 2004; Brennan *et al.* 2006; Takano *et al*. 2007). When assayed directly, their channel permeation was substantial (Fig. 5a) and blocked by octanol (Fig. 5b), consistent with NAD^+ passage through Cx43 “hemichannels” (Bruzzone *et al*. 2001). The areas labeled by NADH (di-sodium and di-potassium salts) were similar to each other and to that of the internal standard dye, but Alexa Fluor 568 labeling almost doubled when assayed in the presence of the tetrasodium salt of

NADPH (Fig. 5a). The stimulatory effect on dye spread of high Na^+ level was confirmed by diffusion of Na^+- or K^+-gluconate into single astrocytes (Fig. 5c). Na^+ loading also elicited an endogenous metabolic response that increased NAD(P)H fluorescence in nearby coupled cells, labeling an area 18-22% that of Alexa Fluor 568 (Fig. 5c). The magnitude of the cation-evoked rise in endogenous NAD(P)H fluorescence in adjacent coupled cells was similar to that in the impaled cell, whereas there was no change in nearby cells that were not coupled (i.e., not dye-labeled, Fig. 5d) to the cation-loaded cell, ruling out contributions of extracellular signaling pathways. These cation-evoked syncytial NAD(P)H responses probably arose from diffusion into coupled cells, stimulating syncytial Na^+, K^+-ATPase activity and ATP demand, causing increased glycolytic flux and a rise in endogenous NADH level.

DISCUSSION

Glucose-6-P is generated by the first irreversible step in the glycolytic pathway and it is an important regulatory metabolite that acts by feedback inhibition of hexokinase. Glucose-6-P is also a 'branch point' metabolite that is further metabolized by different pathways in astrocytes: (i) glycolysis to form pyruvate for energy production and for de novo biosynthesis of the excitatory neurotransmitter glutamate, (ii) pentose phosphate shunt pathway to generate NADPH, a key redox intermediate required for protection against oxidative stress, and (iii) synthesis of glycogen, the only fuel reserve in brain that is located predominantly in astrocytes and turns over more rapidly during sensory stimulation (Hertz *et al*. 2007). Microinjection of glucose-6-P plus allosteric activators of glycolysis has been shown to induce NAD(P)H transients in gap junction-coupled pancreatic and glioma cells, but the substrates transferred were not identified (Thorell *et al*. 1978; Kohen *et al*. 1979). Our data rule out significant glucose-6-P transfer and suggest that retention of glucose-6-P in the cell where glucose is phosphorylated may be essential for fine-tuned pathway flux control; diffusion of NAD(P)H or other metabolites (Figs. 4 and 5) may account for the responses observed by Thorell *et al*. (1978) and Kohen *et al*. (1979). Furthermore, the findings of the present study underscore limitations of label transfer assays using labeled metabolizable tracers that can be converted to other labeled compounds before or after gap junctional transfer and during cell separation procedures (Goldberg *et al.* 1999). The permeant ^{14}C-compounds derived from [^{14}C] glucose-6-P (Tabernaro *et al*. 1996) are unknown, and the model of metabolic interactions among coupled astrocytes (Tabernaro *et al.* 2006) needs to be revised to incorporate restricted diffusion of glucose-6-P.

The structural basis for gating the transfer of hexose-6-phosphates through hemichannels and transcellular pores in astrocytes expressing Cx43, Cx32, and Cx26 is unknown but is not explained by net charge, anionic moiety, molecular size, hydrophobicity, channel blockade by large quantities of competing compounds, ATP/ADP ratio, or astrocyte maturation *in vitro* or *in vivo*. 2-NBDG-6-P, DG-6-P, and glucose-6-P differ in size and hydrophobicity but are not restricted by the presence of a phosphate moiety or its negative charge, since smaller (glyceraldehyde-3-P) and larger (NADH and NADPH) phosphorylated compounds are permeant. Discrimination of molecular trafficking through astrocytic gap junctions is complex because the same channels that blocked transfer of hexose-6-phosphates simultaneously allowed passage of larger and smaller (see Methods) internal standard anionic fluorescent dyes (Figs. 1-4). Poor hexose-6-P transfer was evident over a 100-fold concentration range (0.2-20 mmol/L) for DG-6-P or NBDG-6-P using assay mixtures containing elevated nucleotide levels with ATP/ADP ratios that spanned the range (6 to 0.2) from normal cellular energetics to energy failure. Conceivably, hexose-6-P regulation is achieved by steric properties of the hexose-P and channel pores, since neutral amino acid substitution can block inositol-1,4,5-P_3 transfer through Cx26 channels without reducing Lucifer yellow passage (Beltramello *et al*. 2005). Fluorescent dyes are useful tools but do not predict the fate of endogenous metabolites. Development of rapid, selective, dehydrogenase-linked enzyme assays is a new approach to

assess channel trafficking of unlabeled compounds, and hexose-6-phosphates may be useful probes to evaluate connexin amino acids or domains that govern channel selectivity.

Apparently-discrepant results in our studies in cultured astrocytes and inferior colliculus from adult rat brain and recent studies in immature rat and mouse brain raise the possibility of regional, developmental, connexin, and species differences in connexin channel gating. For example, fluorescence recovery after photobleaching provided indirect evidence for passage of 2-NBDG-6-P through gap junctional channels in Bergmann glia in slices of cerebellum from 12-18 day-old-rats (Barros *et al*. 2009), and connexin36-coupled interneurons that form GABAergic networks in brain (Fukuda *et al*. 2006; Fukuda, 2009) may have different regulatory properties than glial connexins. Rouach *et al.* (2008) recently reported reduced gap junctional spread of 2-NBDG-6-P through astrocytic gap junctions compared to 2-NBDG in slices from 2-4-week-old mice, but the number of NBDG-6-P-labeled cells was higher than that obtained in the presence of carbenoxolone (a gap junction inhibitor), contrasting our finding that the area labeled by hexose-6-phosphates was similar to that obtained by the impermeant internal standard and to those of permeant tracers assayed in the presence of octanol (Figs 1-4). Because apparent spreading of phosphorylated hexoses would occur if some of the parent hexose remained in the injectant we verified the completeness of derivatization reactions for 2-NBDG and [^{3}H]DG. Also, we observed reduced 2-NBDG spreading in the absence of blockade of glucose transporters in our cultured astrocytes (Table 1), whereas Rouach *et al.* (2008) found no effect of cytochalasin-B on 2-NBDG transfer (their Fig. S4). Low glucose transporter levels and a different metabolic phenotype in immature compared to adult brain may contribute to differences obtained in various preparations. During the period prior to and after weaning there are major developmental changes, involving large shifts in glucose and lactate transporter levels and distribution (Cremer *et al*. 1979; Vannucci and Simpson 2003) and conversion from metabolism of lactate, ketone bodies, and glucose during the suckling period to predominately glucose in the adult; these changes arise from up- and down-regulation of many metabolic enzymes and transporters (Cremer 1982; Nehlig 1999, 2004). Immature brain is easier to use in electrophysiological studies, but it is developmentally-active, with marked changes in transport and metabolic capabilities from day to day. Age-dependent differences in glucose and lactate transport and metabolic capability must be taken into account when interpreting the contributions of glucose and alternative fuels to astrocytic and neuronal energetics.

The use of exogenous and endogenous brain imaging tracers to study cellular activity and interactions requires consideration of both the metabolic and syncytial fate of the ‘reporter’ molecules. Retention of radiolabeled DG-6-P in the cell where it is metabolized underscores its usefulness in focal imaging studies (Sokoloff 1986), particularly during brain activation. Because further metabolism of DG-6-P in brain is very limited (Dienel and Cruz 1993), we conclude that DG-6-P is the primary labeled compound retained within the impaled cell. However, phosphoglucomutase can convert DG-6-P to DG-1-P which is an acid labile compound (Dienel *et al*. 1990), and slow hydrolysis of DG-1-P in intracellular acidic compartments would regenerate DG that could diffuse through gap junctions, consistent with the suggestion by Finbow and Pitts (1981) that DG-6-P metabolites may explain its apparent transfer during their long-term assays. In contrast to the DG-6-P and 2-NBDG-6-P, rapid, extensive spreading of downstream metabolites of labeled glucose through astrocytic gap junctions contributes to degradation of focal registration of metabolic activation, even during short, 5 min labeling periods (Ball *et al*. 2007; Dienel and Cruz 2008; Cruz *et al*. 2007). Metabolite dispersal and label release would interfere with studies of focal activation using ^{14}C-, ^{11}C- or ^{13}C-labeled glucose, acetate, and other labeled tracers.

Endogenous NAD(P)H fluorescence is commonly used in fluorescence microscopic assays to evaluate neuron-astrocyte interactions, and percent changes ($\Delta F/F_o$) are typically within the

range from 3-15%, but can be larger with very strong stimuli or abnormal conditions (Shuttleworth *et al*. 2003; Kasischke *et al*. 2004; Brennan *et al*. 2006; Takano *et al*. 2007). Syncytial trafficking of cytoplasmic NAD(P)H may interfere with interpretation of cellular activity, since redox shuttling could reduce the signal in activated, coupled astrocytes compared to nearby uncoupled astrocytes or neurons, causing underestimation of a metabolic response (e.g., it could be reduced by up to a factor of 6, based on NAD(P)H areas in presence and absence of octanol, Fig. 5a,b). Dissipation of astrocytic cytoplasmic responses may be enhanced by cation-dependent up-regulation of gap junctional communication during brain activation.

In conclusion, regulated metabolite trafficking within the astrocytic syncytium appears to be an important component of astrocytic responses to synaptic activity. Enhanced dye transfer by intracellular sodium (Fig. 5) and by extracellular K^+ and glutamate (Enkvist and McCarthy 1994) may link gap junctional communication to synaptic activity, and up-regulation of ion and metabolite trafficking and metabolism in coupled cells by cations may distribute metabolic work from activated perisynaptic astrocytes to the syncytium. Metabolite shuttling may help control local pathway fluxes, distribute the energetic and redox burden arising from transmitter clearance and cation pumping among many astrocytes, and quickly disperse lactate from activated cells to prevent inhibition of glycolysis due to lactate accumulation.

Acknowledgments

This work was supported by National Institutes of Health grants NS36728 and NS47546, Alzheimer Foundation grant IIRG-06-26022, and the University of Arkansas for Medical Sciences Department of Physiology & Biophysics, Graduate School, and Research Council.

REFERENCES

Aller CB, Ehmann S, Gilman-Sachs A, Snyder AK. Flow cytometric analysis of glucose transport by rat brain cells. Cytometry 1997;27:262–268. [PubMed: 9041115]

Araque A, Parpura V, Sanzgiri RP, Haydon PG. Tripartite synapses: glia, the unacknowledged partner. Trends Neurosci 1999;22:208–215. [PubMed: 10322493]

Ball KK, Gandhi GK, Thrash J, Cruz NF, Dienel GA. Astrocytic connexin distributions and rapid, extensive dye transfer via gap junctions in the inferior colliculus: Implications for [^{14}C]glucose metabolite trafficking. J. Neurosci. Res 2007;85:3267–3283. [PubMed: 17600824]

Barros LF, Courjaret R, Jakoby P, Loaiza A, Lohr C, Deitmer JW. Preferential transport and metabolism of glucose in Bergmann glia over Purkinje cells: A multiphoton study of cerebellar slices. Glia 2009;57:962–970. [PubMed: 19062182]2008

Beltramello M, Piazza V, Bukauskas FF, Pozzan T, Mammano F. Impaired permeability to Ins(1,4,5) P_3 in a mutant connexin underlies recessive hereditary deafness. Nat. Cell Biol 2005;7:63–69. [PubMed: 15592461]

Brennan AM, Connor JA, Shuttleworth CW. NAD(P)H fluorescence transients after synaptic activity in brain slices: predominant role of mitochondrial function. J. Cereb. Blood Flow Metab 2006;26:1389–1406. [PubMed: 16538234]

Bruzzone S, Guida L, Zocchi E, Franco L, De Flora A. Connexin 43 hemi channels mediate Ca^{2+}-regulated transmembrane NAD^+ fluxes in intact cells. FASEB J 2001;15:10–12. [PubMed: 11099492]

Cremer JE. Substrate utilization and brain development. J. Cereb. Blood Flow Metab 1982;2:394–407. [PubMed: 6754750]

Cremer JE, Cunningham VJ, Pardridge WM, Braun LD, Oldendorf WH. Kinetics of blood-brain barrier transport of pyruvate, lactate and glucose in suckling, weanling and adult rats. J. Neurochem 1979;33:439–445. [PubMed: 469534]

Cruz NF, Ball KK, Dienel GA. Imaging focal brain activation in conscious rats: Metabolite spreading and release contribute to underestimation of glucose utilization with [^{14}C]glucose. J. Neurosci. Res 2007;85:3254–3266. [PubMed: 17265468]

Dienel GA, Cruz NF. Synthesis of deoxyglucose-1-phosphate, deoxyglucose-1,6-bisphosphate, and other metabolites of 2-deoxy-D-[^{14}C]glucose in rat brain in vivo: influence of time and tissue glucose level. J. Neurochem 1993;60:2217–2231. [PubMed: 8492127]

Dienel GA, Cruz NF. Imaging Brain Activation: Simple Pictures of Complex Biology. Ann. N. Y. Acad. Sci 2008;1147:139–170. [PubMed: 19076439]

Dienel GA, Cruz NF, Mori K, Sokoloff L. Acid lability of metabolites of 2-deoxyglucose in rat brain: implications for estimates of kinetic parameters of deoxyglucose phosphorylation and transport between blood and brain. J. Neurochem 1990;54:1440–1448. [PubMed: 2156023]

Enkvist MO, McCarthy KD. Astroglial gap junction communication is increased by treatment with either glutamate or high K+ concentration. J. Neurochem 1994;62:489–495. [PubMed: 7905024]

Finbow ME, Pitts JD. Permeability of junctions between animal cells. Intercellular exchange of various metabolites and a vitamin-derived cofactor. Exp. Cell Res 1981;131:1–13. [PubMed: 7447983]

Fukuda T, Kosaka T, Singer W, Galuske RA. Gap junctions among dendrites of cortical GABAergic neurons establish a dense and widespread intercolumnar network. J. Neurosci 2006;26:3434–3443. [PubMed: 16571750]

Fukuda T. Network architecture of gap junction-coupled neuronal linkage in the striatum. J. Neurosci 2009;29:1235–1243. [PubMed: 19176831]

Goldberg GS, Lampe PD, Nicholson BJ. Selective transfer of endogenous metabolites through gap junctions composed of different connexins. Nat. Cell Biol 1999;1:457–459. [PubMed: 10559992]

Gross PM, Sposito NM, Pettersen SE, Panton DG, Fenstermacher JD. Topography of capillary density, glucose metabolism, and microvascular function within the rat inferior colliculus. J. Cereb. Blood Flow Metab 1987;7:154–160. [PubMed: 3558498]

Harris AL. Connexin channel permeability to cytoplasmic molecules. Prog. Biophys. Mol. Biol 2007;94:120–43. [PubMed: 17470375]

Hertz L, Peng L, Dienel GA. Energy metabolism in astrocytes: high rate of oxidative metabolism and spatiotemporal dependence on glycolysis/glycogenolysis. J. Cereb. Blood Flow Metab 2007;27:219–249. [PubMed: 16835632]

Hertz L, Peng L, Lai JC. Functional studies in cultured astrocytes. Methods 1998;16:293–310. [PubMed: 10071068]

Iglesias R, Locovei S, Roque A, Alberto AP, Dahl G, Spray DC, Scemes E. P2X7 receptor-Pannexin1 complex: pharmacology and signaling. Am J Physiol Cell Physiol 2008;295:C752–C760. [PubMed: 18596211]

Kasischke KA, Vishwasrao HD, Fisher PJ, Zipfel WR, Webb WW. Neural activity triggers neuronal oxidative metabolism followed by astrocytic glycolysis. Science 2004;305:99–103. [PubMed: 15232110]

Kohen E, Kohen C, Thorell B, Mintz DH, Rabinovitch A. Intercellular communication in pancreatic islet monolayer cultures: a microfluorometric study. Science 1979;204:862–865. [PubMed: 35828]

Moyer JR Jr. Brown TH. Methods for whole-cell recording from visually preselected neurons of perirhinal cortex in brain slices from young and aging rats. J. Neurosci. Methods 1998;86:35–54. [PubMed: 9894784]

Nagy JI, Dudek FE, Rash JE. Update on connexins and gap junctions in neurons and glia in the mammalian nervous system. Brain Res. Rev 2004;47:191–215. [PubMed: 15572172]

Nehlig A. Age-dependent pathways of brain energy metabolism: the suckling rat, a natural model of the ketogenic diet. Epilepsy Res 1999;37:211–221. [PubMed: 10584971]

Nehlig A. Brain uptake and metabolism of ketone bodies in animal models. Prostaglandins Leukot. Essent. Fatty Acids 2004;70:265–275. [PubMed: 14769485]

Nimmerjahn A, Kirchhoff F, Kerr JN, Helmchen F. Sulforhodamine 101 as a specific marker of astroglia in the neocortex in vivo. Nat. Methods 2004;1:31–37. [PubMed: 15782150]

Rouach N, Koulakoff A, Abudara V, Willecke K, Giaume C. Astroglial metabolic networks sustain hippocampal synaptic transmission. Science 2008;322:1551–1555. [PubMed: 19056987]

Shuttleworth CW, Brennan AM, Connor JA. NAD(P)H fluorescence imaging of postsynaptic neuronal activation in murine hippocampal slices. J. Neurosci 2003;23:3196–3208. [PubMed: 12716927]

Sokoloff, L. Cerebral circulation, energy metabolism, and protein synthesis: General characteristics and principles of measurement. In: Phelps, M.; Mazziotta, J.; Schelbert, H., editors. Positron Emission Tomography and Autoradiography: Principles and Applications for the Brain and Heart. Raven Press; New York: 1986. p. 1-71.

Speizer L, Haugland R, Kutchai H. Asymmetric transport of a fluorescent glucose analogue by human erythrocytes. Biochim. Biophys. Acta 1985;815:75–84. [PubMed: 4039191]

Suadicani SO, Brosnan CF, Scemes E. P2X7 receptors mediate ATP release and amplification of astrocytic intercellular Ca^{2+} signaling. J. Neurosci 2006;26:1378–1385. [PubMed: 16452661]

Tabernero A, Giaume C, Medina JM. Endothelin-1 regulates glucose utilization in cultured astrocytes by controlling intercellular communication through gap junctions. Glia 1996;16:187–195. [PubMed: 8833189]

Tabernero A, Medina JM, Giaume C. Glucose metabolism and proliferation in glia: role of astrocytic gap junctions. J. Neurochem 2006;99:1049–1061. [PubMed: 16899068]

Takano T, Tian GF, Peng W, Lou N, Lovatt D, Hansen AJ, Kasischke KA, Nedergaard M. Cortical spreading depression causes and coincides with tissue hypoxia. Nat. Neurosci 2007;10:754–762. [PubMed: 17468748]

Thorell B, Kohen E, Kohen C. Metabolic rates and intercellular transfer of molecules in cultures of human glia and glioma cells. Med. Biol 1978;56:386–392. [PubMed: 32440]

Vannucci SJ, Simpson IA. Developmental switch in brain nutrient transporter expression in the rat. Am. J. Physiol. Endocrinol. Metab 2003;285:E1127–E1134. [PubMed: 14534079]

Volterra A, Meldolesi J. Astrocytes, from brain glue to communication elements: the revolution continues. Nat. Rev. Neurosci 2005;6:626–640. [PubMed: 16025096]

Ye ZC, Wyeth MS, Baltan-Tekkok S, Ransom BR. Functional hemichannels in astrocytes: a novel mechanism of glutamate release. J. Neurosci 2003;23:3588–3596. [PubMed: 12736329]

Zündorf G, Kahlert S, Reiser G. Gap-junction blocker carbenoxolone differentially enhances NMDA-induced cell death in hippocampal neurons and astrocytes in co-culture. J. Neurochem 2007;102:508–521. [PubMed: 17403140]

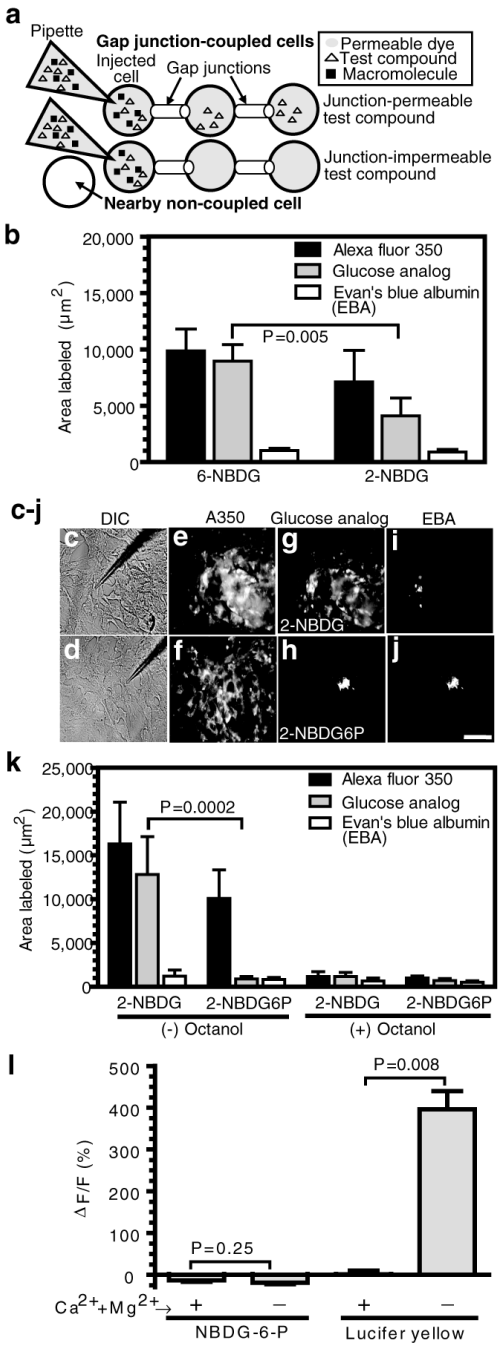

Figure 1. Restricted gap junctional and 'hemichannel'- or pannexin-mediated transfer of NBDG-6-phosphate in cultured astrocytes

(a) Schematic illustration of gap junction transfer assays shows single astrocytes impaled with a micropipette containing (i) a gap junction-permeable fluorescent dye that serves as an internal standard to identify coupled cells (denoted by shading; the non-coupled cell has a white background) and against which the area labeled during the 10 min diffusion interval by test compounds is compared (i.e., to account for heterogeneous coupling and variability among batches of cells); (ii) a test compound; and (iii) a gap junction-impermeable macromolecule to identify the impaled cell. (b) Relative labeling by 2-NBDG and 6-NBDG (area labeled by test compound divided by the area labeled by the channel permeant internal standard for each

impaled cell) was used to identify significant differences (t test; n=5/group). (c-j) Representative differential interference contrast (DIC) images of astrocytes impaled with a micropipette (c, d) and fluorescence images after diffusion of 2-NBDG (e, g, i) or 2-NBDG-6-phosphate (f, h, j) plus permeant (Alexa Fluor 350, A350) and impermeant (Evan's blue albumin, EBA) internal standards. The scale bar = 50 μm and applies to all panels. (k) Areas labeled in the absence (-) or presence (+) of octanol, a gap junction blocker. P values for indicated comparisons (t test) were determined using transformed ratios (test compound/ internal standard); n = 31 and 11 for NBDG and n = 20 and 6 for NBDG-6-P in the absence and presence of octanol, respectively. (l) Percent change of fluorescence in astrocytes pre-loaded with NBDG-6-P after 25 min perfusion with medium containing (+) or nominally lacking (-) Ca^{2+} and Mg^{2+}, which opens 'hemichannels' and pannexin pores (left panels), and the subsequent 5 min exposure of the same astrocytes to Lucifer yellow in the presence or absence of divalent cations followed by a 20 min wash with divalent cation-containing perfusate (right panels). P values (t test) are for indicated comparisons (n = 8, 11, 6, 14 for the respective +cation and -cation groups for NBDG-6-P and Lucifer yellow).

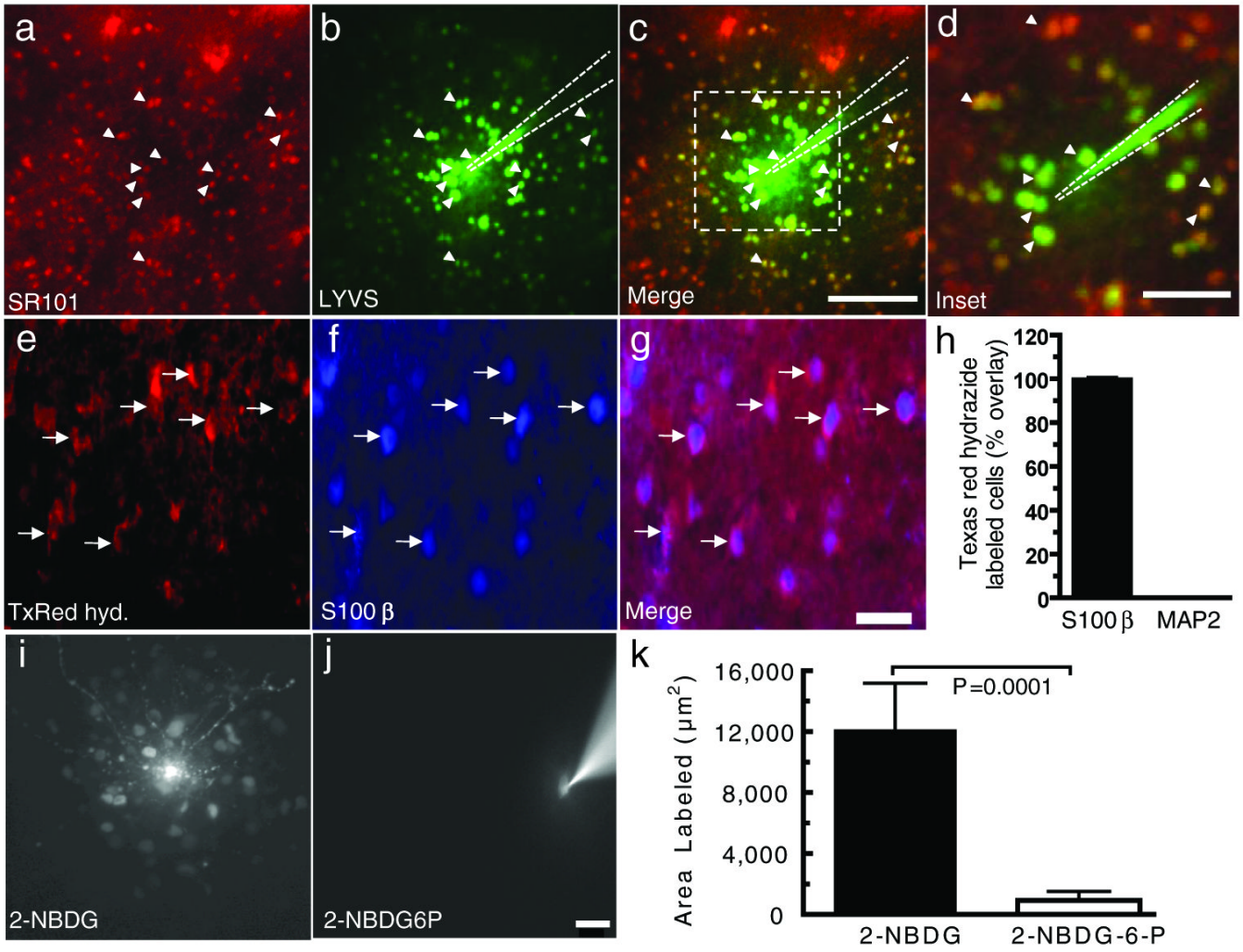

Figure 2. Retention of 2-NBDG-6-P in highly-coupled, sulforhodamine 101-positive astrocytes in slices of inferior colliculus from adult rat brain

One of the cells labeled by slice incubation in sulforhodamine 101 (SR101) (a) was impaled with a micropipette (b) to identify gap-junction coupled cells labeled by diffusion of Lucifer yellow VS (LYVS; color coded green). (c) The merged image of panels a and b illustrates extensive overlap (yellow) of SR101 (red) and LYVS (green) labeling; the scale bar represents 100 μm and applies to panels a-c. Note that the intensity of the Lucifer yellow-labeled cells near the impaled cell was so high that overlay with SR101 was obscured. The dashed box in (c) outlines the inset shown at higher magnification (d; scale bar represents 40 μm). Dashed lines in b-d denote the pipette location, and arrowheads identify the same selected SR101-positive astrocytes. (e) Slices of inferior colliculus were labeled with a fixable analog of SR101, Texas red hydrazide (TxRed hyd), and immunostained for an astrocyte marker, S100β (f) or a neuronal marker, MAP2 (data not shown); the merged image (g) shows co-registration of Texas red with S100β-positive cells; arrows identify the same cells in panels e-g. The scale bar = 25 μm in g, and applies to panels e-g. (h) Percent of Texas red-labeled cells (n = 370) assayed in 10 brain slices that were S100β-positive; none were MAP2-positive. Cells labeled by 2-NBDG (i) and 2-NBDG-6-phosphate (2-NBDG6P) (j) after a single SR101-labeled astrocyte was impaled and tracer diffused into the cell for 10 min; scale bar = 25 μm in i and j. (k) Area labeled by 2-NBDG (n=9) and 2-NBDG6P (n=10) in brain slices (The P value was determined with the t-test).

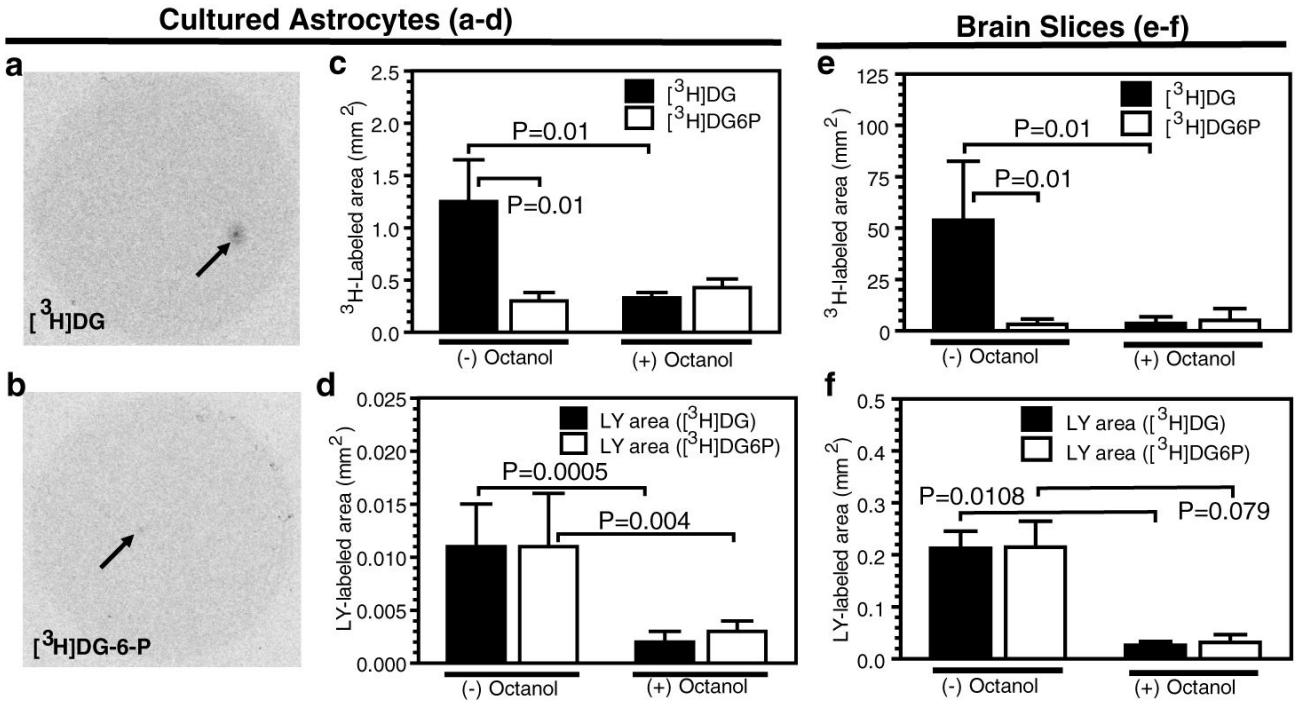

Figure 3. Channel permeation of [^{3}H]deoxyglucose (DG) but not [^{3}H]DG-6-P

Autoradiographic images of ^{3}H labeling after diffusion of Lucifer yellow VS (LY) plus [^{3}H] DG (a) or [^{3}H]DG-6-P (b) into a single cultured astrocyte for 10 min; arrows indicate the injection sites. The ^{3}H-labeled areas (c, e) and Lucifer yellow-labeled areas (d, f) in cultured astrocytes (c, d) and in astrocytes in brain slices of the inferior colliculus from adult rats (e, f) are mean values determined in the absence (-) or presence (+) of octanol to block gap junctions. P values for indicated comparisons were determined by ANOVA and Tukey's test or t test; the numbers of assays per group are as follows. For cultured astrocytes: panel c, [^{3}H]DG, n = 13; [^{3}H]DG-6-P, n = 13; octanol-treated groups, n = 4/group; panel d, Lucifer yellow-labeled assays: [^{3}H]DG cells, n = 8; [^{3}H]DG-6-P cells, n=9; octanol-treated groups, n=3. For brain slices: panel e, [^{3}H]DG, n = 13; [^{3}H]DG-6-P, n = 14; octanol-treated slices, n=4/group; panel f, Lucifer yellow-labeled areas in slices labeled [^{3}H]DG, n = 4 or [^{3}H]DG-6-P, n = 5; octanol-treated slices, n=2/group (for these two groups the vertical bars denote the range).

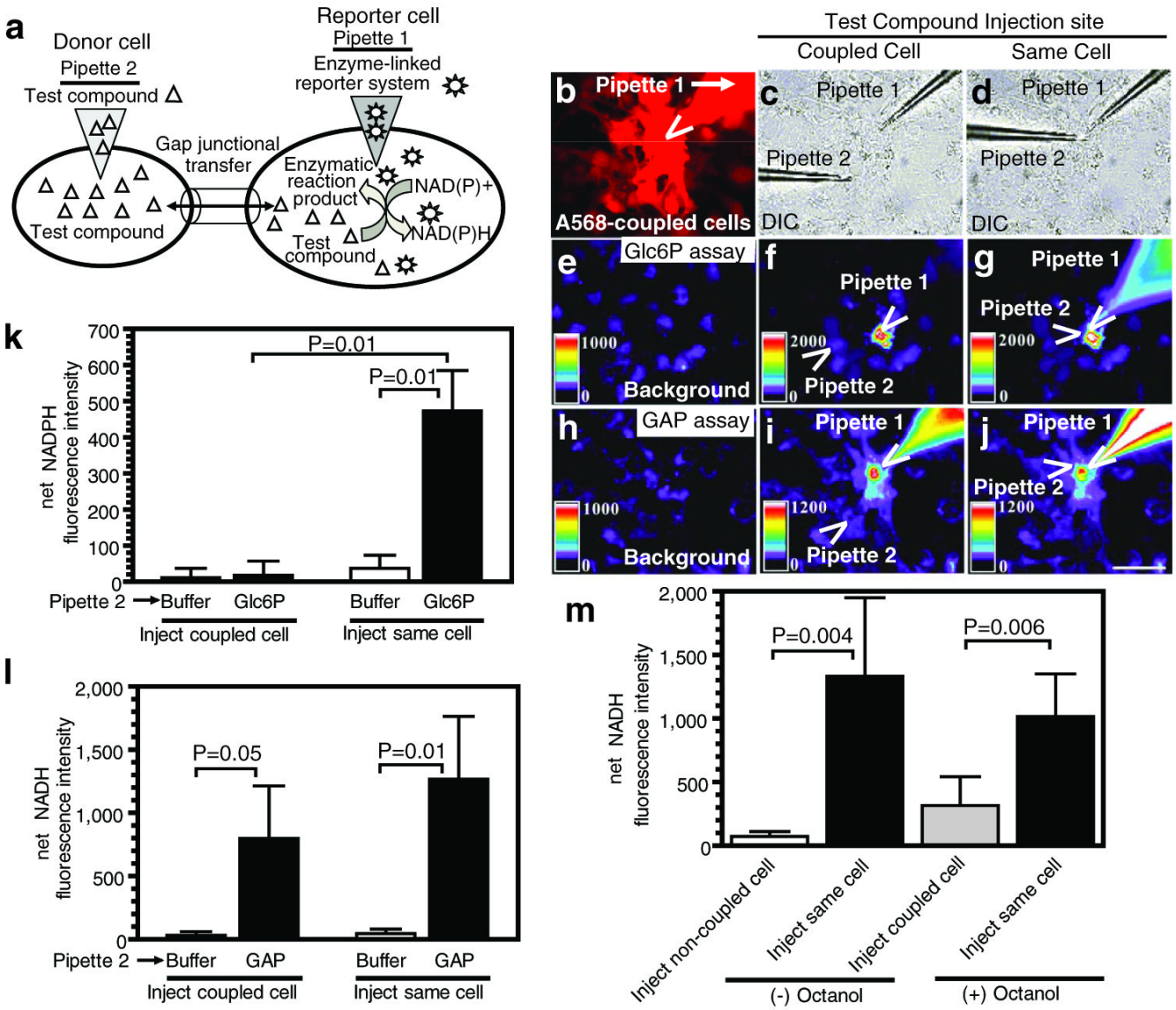

Figure 4. Novel, single-cell enzymatic assays for gap junctional trafficking of unlabeled glycolytic intermediates

(a) Schematic of the principle of dehydrogenase-linked fluorescence assays for channel permeation of unlabeled metabolites. The enzymatic reaction mixture plus a permeant fluorescent dye are introduced into an impaled cell; the test compound is diffused into a dye-labeled coupled cell, and its transfer to the reporter cell and oxidation generates NAD(P)H fluorescence. Representative assays for glucose-6-phosphate (Glc6P) and glyceraldehyde-3-phosphate (GAP) transfer among astrocytes are illustrated in panels b-j; the scale bar in j represents 50 μm and applies to all panels. Cultured astrocytes are visualized under differential interference microscopy (DIC), a single astrocyte is impaled with pipette 1 containing the reporter system plus Alexa Fluor 568 (A568) (c) and coupled cells visualized (b). Then a dye-labeled donor cell located 50 ± 5 μm from the reporter is impaled with pipette 2 (c) containing the test compound or buffer (a control for endogenous metabolic responses arising from mechanical perturbation of the cell). To verify that the reporter system works, pipette 2 is next withdrawn from the donor cell and inserted into the reporter cell containing pipette 1 (denoted as ‘same cell’ in d, g, j) and the fluorescence is again measured in the reporter cell. Because

the pipettes are not fluorescent, the locations of the pipette tips visible in panels c and d are identified by open arrowheads in panels b, f, g, i, j. Typical assays for glucose-6-phosphate (e-g) and glyceraldehyde-3-phosphate (h-j) involve sequential determination of background fluorescence before pipette 1 insertion (e, h), reporter cell fluorescence before and 1 min after insertion of pipette 2 in a coupled donor cell (f, i), and reporter cell fluorescence at 1 min after removal of pipette 2 from the coupled cell and its insertion into the reporter cell that also contains pipette 1 (denoted as same cell) (d, g, j). Note that metabolism of endogenous substrates in 7 of 15 reporter cells increased their ΔF/F by 142-699% after insertion of pipette 1 containing the Glc6P assay mixture, whereas 8 reporter cells had <42% increase in ΔF/F; the mean ± SD change in ΔF/F was 207 ± 239, n=15. The reporter cell shown in panel (f) is an example of an 'endogenous substrate responder' to insertion of pipette 1; it had a higher NADPH fluorescence compared to the surrounding cells (f) and to the background (e). However, the *net fluorescence change* in all reporter cells at 1 min after impaling a coupled donor cell with pipette 2 compared to that after insertion of pipette 1 (c, f) was very small (k, left two bars). Direct insertion of pipette 2 containing glucose-6-phosphate into the reporter cell (d, g) caused the net fluorescence to increase in the reporter cell and reporter pipette (k, right two panels). In the glyceraldehyde-3-phosphate assays (h-j), both the injected cell and pipette 1 had high NADH fluorescence when glyceraldehyde-3-phosphate diffused from pipette 2 into a coupled cell (i), and diffusion of substrate directly into the reporter cell markedly increased NADH fluorescence in pipette 1 (j); cells surrounding the reporter cell (i, j) have higher fluorescence than background (h). Note that 11 of 20 GAP reporter cells increased ΔF/F by 228-1229% after insertion of pipette 1 containing the GAP assay mixture, whereas 9 reporter cells had <148% increase in ΔF/F (the mean ± SD change in ΔF/F was 452 ± 456; n=20 cells); these increases reflect metabolism of endogenous substrates. Additional control assays (m, left two panels) demonstrate that GAP does not evoke an increase in net NADH fluorescence in the reporter cell when pipette 2 is inserted into a non-coupled astrocyte (i.e., not labeled by Alexa Fluor 568). The reporter system is, however, still responsive to substrate after withdrawal of pipette 2 from the uncoupled cell and its insertion into the reporter cell. Pre-treatment (+) of astrocytes with octanol markedly reduced the reporter cell fluorescence response when GAP was inserted into a coupled cell but octanol did not block the enzyme assay when pipette 2 was in the same reporter cell. Values are means of net NADPH fluorescence intensities; P values are shown for the indicated comparisons (ANOVA and Tukey's test or t test) for the following numbers of samples: panel k: n = 10 for Glc6P, n = 5 for buffer controls; panel l: n = 9 for GAP, n = 5 for buffer controls; panel m: n = 5/group.

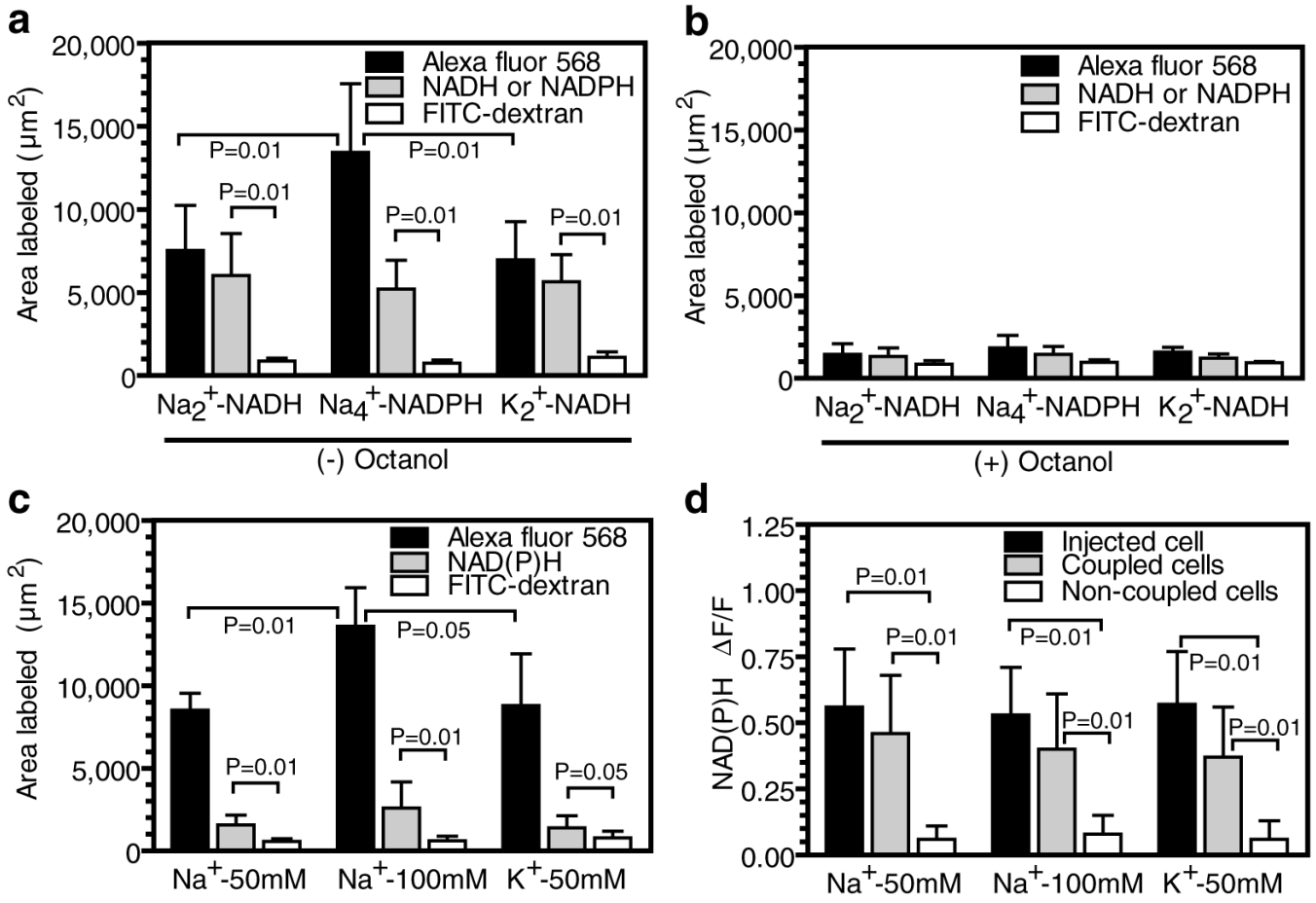

Figure 5. Syncytial trafficking of redox compounds and stimulation of dye spread by Na^+

Areas labeled by 5 mmol/L Alexa Fluor 568 (A568), 25 mmol/L NADH (disodium, n=13 or dipotassium, n=10 salts), 25 mmol/L NADPH (tetrasodium salt, n = 13), and 4% (weight/volume) FITC conjugated dextran before (**a**) or after (**b**) octanol treatment (0.6 mM for 10 min, n = 5/group). (**c**) Area labeled by 5 mmol/L A568, endogenously-produced NAD(P)H and 4% FITC-conjugated dextran after insertion of a pipette containing the indicated concentrations of Na^+ or K^+ (gluconate) in the pipette solution (n = 4/group). (**d**) Relative increase in fluorescence of endogenous NAD(P)H in cells impaled with a micropipette containing the indicated concentrations of Na^+ or K^+ (gluconate) compared to the evoked changes in NAD(P)H fluorescence in nearby gap junction-coupled and non-coupled cells. For 50 mmol/L Na^+, n = 8, 16, or 21 for the injected, coupled, and non-coupled cells, respectively. For 100 mmol/L Na^+, n = 9, 17, or 24 for the injected, coupled, and non-coupled cells, respectively. For 50 mmol/L K^+, n = 7, 12, or 21 for the injected, coupled, and non-coupled cells, respectively. P values are given for the indicated comparisons (ANOVA and Tukey's test or t test).

Table 1
Influence of glucose transporter blockade and ADP on fluorescent dye transfer

Tracer	Cytochalasin B in perfusion solution (μmol/L)	Nucleotide (concentration in pipette solution, mmol/L)	Area labeled (μm^2)
Alexa Fluor 350	10	ATP (22)	16,250 ± 4,756 (n = 31)
	10	ADP (22)	15,518 ± 5,180 (n = 15)
Lucifer Yellow VS	0	ATP (2) + GTP (0.5)	14,703 ± 2,605 (n = 21)
	10	ADP (22)	11,385 ± 2, 387 [a] (n = 8)
2-NBDG	0	ATP (22)	5,614 ± 850 (n = 4)
	10	ATP (22)	12,849 ± 4,309 [b] (n = 31)
	10	ADP (22)	12,088 ± 4,328 [b] (n = 15)
2-NBDG-6-P	0	ADP (20) + ATP(2)	891 ± 153 (n = 4)
	10	ADP (20) + ATP (2)	882 ± 271 (n = 20)

Cultured astrocytes were perfused with 10 mmol/L glucose plus 10mmol/L pyruvate in artificial CSF with or without cytochalasin B for 10 min prior to and throughout the dye transfer assays. Single cells were then microinjected with eitherthe 2-NBDG phosphorylation reaction mixture plus Alexa Fluor 350 with or without added hexokinase to produce 2-NBDG-6-P, and labeled areas were measured after 10 min diffusion (see Methods) or Lucifer yellow-containing solution. After completion of the phosphorylation reaction, the hexokinase-containing reaction mixtures contained (concentrations in mmol/L) 20 2-NBDG-6-P + 20 ADP + 2 ATP. Mixtures without hexokinase contained 20 2-NBDG + 22 ATP or 22 ADP. Values are means ± SD for the number of cells indicated in parentheses.

[a] P=0.0118 (t test) compared to 0 cytochalasin B in perfusate.

[b] P=0.01 (ANOVA, Tukey's test) compared to 0 cytochalasin B in perfusate.